

Measurements of current-voltage-induced heating in the Al/SrTiO_{3-x}N_y/Al memristor during electroformation and resistance switching

A. Shkabko,^{1,a)} M. H. Aguirre,¹ I. Marozau,² T. Lippert,² and A. Weidenkaff¹

¹Solid State Chemistry and Catalysis, Empa, Ueberlandstrasse 129, 8600 Duebendorf, Switzerland

²Paul Scherrer Institut, 5232 Villigen PSI, Switzerland

(Received 21 July 2009; accepted 2 September 2009; published online 15 October 2009)

Heating of the Al/SrTiO_{3-x}N_y/Al memristor is characterized during electroformation and switching of the resistances. The electrode with the higher voltage potential is heated to higher temperatures than the electrode with the lower potential, suggesting a reversible (nonstable) displacement of the anions in a low voltage region ($|V| < \pm 3$ V). Application of a threshold voltage appropriate for resistance switching ($|V| \geq \pm 3$ V) facilitates migration of anions to the anode interface and increases the local anode temperature to a maximum of 285 °C. The hysteretic I - V curves are discussed taking into account tunnel barrier formation/break and inhomogeneous Schottky barrier modification at the anode interface. © 2009 American Institute of Physics. [doi:10.1063/1.3238563]

Resistance switching in some ceramic perovskites, for example, SrTiO₃ (Ref. 1) is assigned to ion/vacancy migrations, which we believe are strongly related to the electromigration process.² The migration of the ions and its flux J is an electrocurrent induced process given by the Huntington and Grone theory³ as

$$J = \frac{D_0 N e (Z_{el}^* + Z_{wd}^*) \rho \cdot j}{k_B T} e^{-E_a/kT}, \quad (1)$$

where D_0 is the diffusion constant, k_B —the Boltzmann constant, e —electron charge, N —the density of atoms, Z_{el}^* —the charge number representing electrostatic field force, Z_{wd}^* —the charge number representing electron wind force, ρ —the electrical resistivity of the material, j —the electrical current density, E_a —the activation energy, and T —the absolute temperature. For conducting samples (metals) the electron wind force must, according to the theory, be higher than the electrostatic force ($Z_{wd}^* > Z_{el}^*$),² resulting in mass (atomic) transport mostly due to the high density of electronic current interacting with atoms. By tuning the concentration and the diffusion activation energy of mobile ions in SrTiO_{3-x}N_y, the ionic migration can be varied. Furthermore, as shown recently,⁴ the fabrication of additional stacking fault defects in SrTiO_{3-x}N_y facilitates electroformation and resistance switching.

Another aspect of the ion transport [Eq. (1)] is the change in ionic conductivity by temperature variations. Even without additional external heating, electromigration itself is a thermally assisted process. Recently, some works showed the importance of Joule heating during resistance switching;^{5,6} however, the real temperature of the memristors has not been reported. Since the electromigration is the result of the combination of thermal and electrical effects on the atomic diffusion,² it is important to know how the electroformation and switching of the memristor are coupled together with the localized heating of the Al/SrTiO_{3-x}N_y/Al.

To synthesize the oxynitride crystal, commercially available (CRYSTEC) SrTiO₃ (100) single crystal grown by Verneuil method were cut and plasma treated in order to incor-

porate nitrogen in the perovskite structure.⁷ Plasma treatments were performed in a quartz tube in the microwave oven under the 125 ml/min ammonia flow following the procedure described elsewhere.^{4,8}

In order to achieve resistance switching [Fig. 1(a)], the voltage V was swept in cycles: 0 V → maximum positive voltage in V^+ contact → maximum negative voltage → 0 V, while the current I was measured in the same manner as previously reported for Al/SrTiO_{3-x}N_y/Al.⁴ The IR emission was acquired by the Jade camera to study the temperature distribution on the sample/contacts during the electroformation and switching of the resistance states [Fig. 1(b)]. The electrical power ($P=IV$) is preferentially dissipated at the virtual anode (VA) [VA, area A, Fig. 1(b)] and virtual cathode (VC) (VC, area B) due to the Schottky barrier formation on the Al/SrTiO_{3-x}N_y interfaces and order of magnitudes higher interface resistances.

For the maximum of +1 V applied voltage, the VA of the Al/SrTiO_{3-x}N_y/Al was heated about 3–5 °C more than the VC [Fig. 2(a)]. The reversal of the polarity symmetrically heats VC 3–5 °C more than VA. This heating has no major influence on the linearity of the I - V curves and the stability of the resistances confirms the symmetry of Al/SrTiO_{3-x}N_y/Al. However, the fact of higher heating of VA at +1 V and symmetrical heating of VC at –1 V requires careful considerations. As expected, for highly doped SrTiO_{3-x}N_y the Schottky-like Al/SrTiO_{3-x}N_y contacts are nearly Ohmic with a small Schottky barrier height prior the electroformation process. This allows to denote the

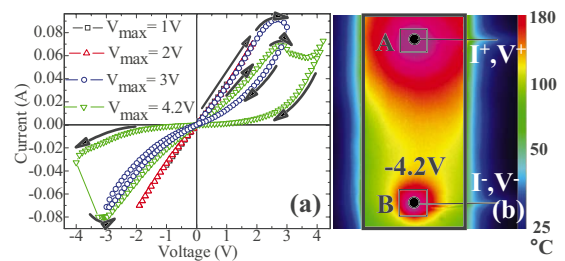


FIG. 1. (Color online) (a) Electroformation I - V characteristics and resistance switching of Al/SrTiO_{3-x}N_y/Al for $V_{max} = \pm 1$ V; ± 2 , ± 3 , and ± 4.2 V. (b) Temperature distributions of the memristor (top view) acquired at -4.2 V.

^{a)}Electronic mail: andrey.shkabko@empa.ch.

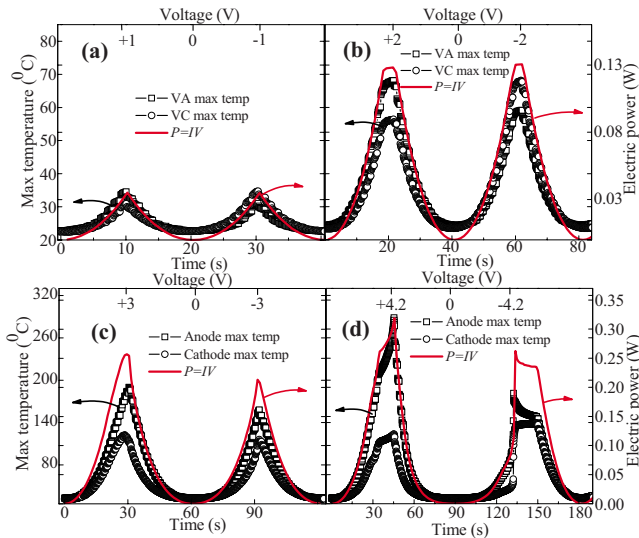


FIG. 2. (Color online) Maximum temperatures of electrodes during electroformation and switching acquired for (a) $V_{\max} = \pm 1$ V, (b) $V_{\max} = \pm 2$ V, (c) $V_{\max} = \pm 3$ V, and (d) $V_{\max} = \pm 4.2$ V.

Al/SrTiO_{3-x}N_y/Al system as a back-to-back Schottky metal-semiconductor-metal device⁹ (Fig. 1 of SI).⁸ Essentially, the Schottky barrier at these interfaces consists of inhomogeneous Schottky barriers profiles due to the presence of regions with stacking faults defects and a nearly defect-free perovskite structure at the surface of the SrTiO_{3-x}N_y.^{10,11} The currents flow through individual patches represented as defects and defect-free regions of various sizes. However, the conductivities and Schottky barriers heights at the stacking faults defects, as well as their concentrations and distributions, require further studies in order to apply a theoretical model (for example, Tung's model¹⁰) which describes thoroughly the electronic current through the metal-semiconductor interfaces.

It is known from the band diagrams of metal-semiconductor-metal junctions operated at comparably low current densities, that an application of positive bias to one of the metals results in a decrease in the potential drop for electrons at this interface. This reveals lower heat dissipation compared with that for the negative bias.¹² However, at higher current densities of 4.9×10^3 A/cm² (+1 V), an electron wind/current impacts the crystal structure and together with electrostatic field force cause local (at the interface) displacement of anions to the positively biased interface. However, maximum of 1V is not sufficient for irreversible anion displacements. Thus, possible reasons of this recovery could be the low electric current density j [Eq. (1)], low electrostatic force and relaxation (back diffusion) of anions to their initial positions.¹³ Thereby, the linear (Ohmic) behavior does not change when sweeping the IV with a maximum voltage of 1V.

A similar temperature difference of $14\% \pm 1\%$ (10 °C) between VA and VC can be measured at 2 V maximum applied voltage [Fig. 2(b)], along with an increased maximum current density of 9.8×10^3 A/cm². A voltage increase in up to +3 V with a maximum current density of 1.3×10^4 A/cm² heats VA 34% more than VC during the positive IV [Fig. 2(c)]. Additionally, the first drop of the conductivity occurs, as shown in Fig. 1(a). Applying a voltage of -3 V initially also heats VA to 25% more than VC which was not observed at lower voltages (<3 V). Thus, the applica-

tion of a 3 V → -3 V cycle irreversibly increase the resistance of the Al/SrTiO_{3-x}N_y and this first hysteresis essentially breaks the symmetry.¹⁴ The break of symmetry means that VA and VC are not interchangeably heated by a change in the polarity, and any further $I-V$ curves measurements are electrode dependant. It is noteworthy that independently of the applied voltage polarity and the choice of the contact, the first switching event appears on VA, and the definition of “anode” is given to the electrode where the first voltage pulse changes the low resistance state (LRS) to high resistance state (HRS).

In order to stabilize the switching and increase the $R_{\text{HRS}}/R_{\text{LRS}}$ ratio, another cycle with +4.2 V maximum is applied. The consequence of the high voltage (+4.2 V) application is the electromigration at the anode interface and an increase in the local maximum temperature of the anode to 285 °C at a peak voltage of 4.2 V, which is 56% higher than the T at the cathode. Similarly to the 3 V cycle, the anode is also heated more during the HRS to LRS switching. At the moment of HRS to LRS switching, the temperatures of the anode and cathode are the same ($T=150$ °C) which makes the interface resistances of both interfaces after switching equal to each other. The difference between cathode and anode as well as inability to exchange the anode and cathode and vice versa during this switching is in the limiting compliance current (-0.085 A) during the change in the resistance state from HRS to LRS. Such current limit prevents the complete symmetrical oxidation of the cathode but still allows a reduction of the anode interface setting the resistance of the anode back to LRS. It can be concluded that during the process of electroformation as well as throughout the switching process, the compliance current limits the electromigration process and thus the oxidation of the cathode, which is important for stable and reversible switching. Without this limitation pinched hysteresis is impossible to realize (Fig. 2 of SI).⁸

The process of memristor operation can be modeled using known equivalent circuit elements and taking into account electromigration where electrons and ions are involved. Prior to electroformation the n -type perovskite with attached Al contacts form Schottky barriers with symmetric barrier heights ϕ_b and a depletion thickness w [Fig. 3(a)]. An application of voltages as high as 2 V, with a current flow of up to 9.8×10^3 A/cm², does not significantly change the stability of the resistance state. However, high density of electron current and electrostatic forces reversibly displace anions to positively biased interfaces causing higher heating.

An increase in the highest applied voltage to +3 and +4.2 V with a maximum current flow of up to 1.3×10^4 A/cm² destroys the symmetry of the Al/SrTiO_{3-x}N_y/Al, especially at the anode interface. The positive anode presumably attracts the negative ions, O²⁻ and N³⁻, at the highest current flows, forming an oxide/oxy-nitride barrier layer which has a lower electrical conductivity, and thus increasing the depletion layer thickness ($w_1 > w$) and the barrier height ($\phi_{b1} > \phi_b$) for the electrons [Fig. 3(b)].

Having an overall small Schottky barrier height on the cathode interface, where changes of the resistances are negligible, the Al/SrTiO_{3-x}N_y/Al memristors can be considered as metal-insulator-semiconductor (MIS) capacitors,¹² where M is the Al anode, I is the nonconducting SrTiO_{3- δ :N} layer,

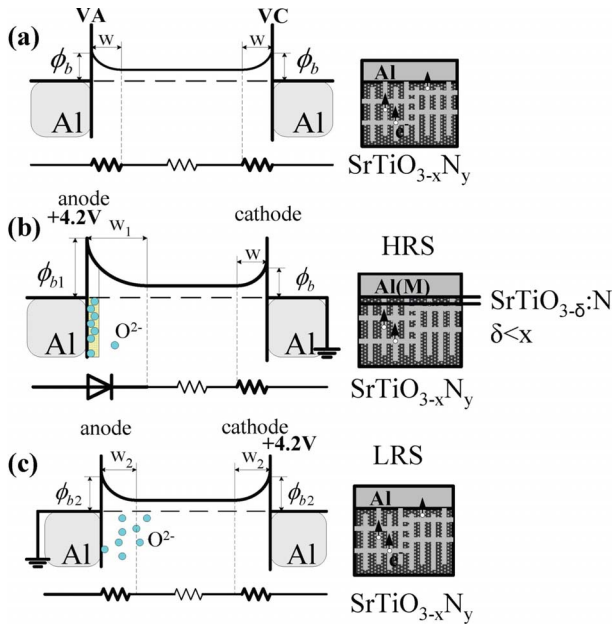


FIG. 3. (Color online) (a) Energy band diagrams and equivalent electric circuit and of the Al/SrTiO_{3-x}N_y/Al prior to *I-V* measurements. (b) Equivalent electric circuit and energy band diagrams in thermal equilibrium of the Al/SrTiO_{3-x}N_y/Al after applying a voltage of +4.2 V to one of the contacts (anode). (c) Equivalent electric circuit and energy band diagrams in thermal equilibrium of the Al/SrTiO_{3-x}N_y/Al after applying a voltage of -4.2 V to the opposite contact (cathode).

and S is the SrTiO_{3-x}N_y (with $x > \delta$) [Fig. 3(b)]. It is known for Si-SiO₂ that an increase in the insulator layer to more than 7 nm decreases the carrier transport thus representing a conventional MIS capacitor.¹² However, between 1 nm (Schottky-barrier diode) and 7 nm (MIS capacitor) different tunneling mechanisms such as Fowler-Nordheim tunneling, direct tunneling, etc., exist, depending on the thickness of the oxide layer.¹² At the moment of the LRS to HRS switch of the Al/SrTiO_{3-x}N_y/Al resistance, the thickness of the oxide/oxy-nitride barrier at the anode interface increases with increasing time (Fig. 3 of SI) (Ref. 8) and the maximum applied voltage. In addition, inhomogeneous Schottky barriers have also to be taken into account due to local variations of the barrier potential caused by mobile anions. Both models, MIS and modification of inhomogeneous Schottky junctions, of electric current are based on a thermionic-emission model. For an estimation of the barrier height, the standard thermionic-emission equation for Schottky barriers at the anode interface is used, i.e., when the electronic current flows in forward direction: $\phi_{b1} = (k_B T / e) [A^{**} T^2 / J_0]$, where $A^{**} = 156 \text{ A/cm}^2 \text{ K}$ is the Richardson constant for SrTiO₃,¹⁵ and J_0 is the saturation current as extrapolated from the current density at zero voltage. The estimated values of the Schottky barrier height increase with the applied voltages, reaching $\phi_{b1} \sim 0.48 \text{ eV}$ after applying +4.2 V (Fig. 4). This is in good agreement with the calculated and theoretically predicted values for the Schottky barrier height of $\sim 0.53 \text{ eV}$ in Al/SrTiO₃ junctions.¹⁶

The application of -4.2 V negative voltage leads to a similar breakdown of the diode by current-voltage-induced and thermally assisted electromigration of anions to their initial positions. This decreases the barrier height ($\phi_{b1} > \phi_{b2}$) and the depletion layer thickness ($w_2 < w_1$) restoring a stable

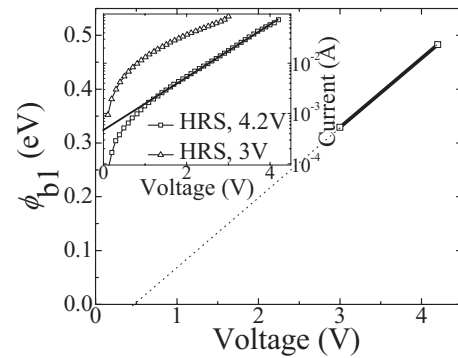


FIG. 4. Calculated Schottky barrier height in HRS after application of +3 and +4.2 V with the dotted line as a guide for the eyes. The inset shows the forward current characteristics for the HRS of the Al/SrTiO_{3-x}N_y/Al memristor.

LRS with linear *I-V* characteristics in the voltages range $< \pm 3 \text{ V}$ [Fig. 3(c)].

Summarizing, the application of a high positive voltage (+3 V and higher) moves the ions to the anode interface by a current-voltage-induced and thermally assisted combination of processes. The formation of the anionic rich layer at the interface is represented by a tunnel diode with inhomogeneous Schottky barrier heights resulting in an average estimated barrier height of $\sim 0.48 \text{ eV}$. This is in good agreement with theoretically predicted values of Al on SrTiO₃.¹⁶ The application of a negative voltage (-3 V and higher) repels ions from the anode interface. In order to keep the memristor in a hysteric regime, the compliance current has to limit the electromigration while the resistance switches from HRS to LRS. This prevents the cathode from oxidation, making Al/SrTiO_{3-x}N_y/Al operating as a memristor.

The authors thank S. Furer, V. Raineri, F. La Mattina, I. Riess, and L. Gauckler for fruitful remarks and discussions, ETHZ-EMEZ for TEM facilities, and E. Hack for IR camera. The work was supported by Swiss National Science Foundation NCCR MaNEP.

¹K. Szot, W. Speier, G. Bihlmayer, and R. Waser, *Nature Mater.* **5**, 312 (2006).

²K. N. Tu, *J. Appl. Phys.* **94**, 5451 (2003).

³H. B. Huntington and A. R. Grone, *J. Phys. Chem. Solids* **20**, 76 (1961).

⁴A. Shkabko, M. H. Aguirre, A. Weidenkaff, I. Marozau, and T. Lippert, *Appl. Phys. Lett.* **94**, 212102 (2009).

⁵M. Janousch, G. I. Meijer, U. Staub, B. Delley, S. F. Karg, and B. P. Andreasson, *Adv. Mater. (Weinheim, Ger.)* **19**, 2232 (2007).

⁶S. B. Lee, S. C. Chae, S. H. Chang, J. S. Lee, S. Park, Y. Jo, S. Seo, B. Kahng, and T. W. Noh, *Appl. Phys. Lett.* **93**, 252102 (2008).

⁷A. Shkabko, M. H. Aguirre, I. Marozau, M. Dobeli, T. Lippert, M. Mallepell, and A. Weidenkaff, *Mater. Chem. Phys.* **115**, 86 (2009).

⁸See EPAPS supplementary material at <http://dx.doi.org/10.1063/1.3238563> for synthesis, characterization, and figures.

⁹A. J. Moulson and J. M. Herbert, *Electroceramics Materials, Properties, Applications* (Wiley, New York, 2003).

¹⁰R. T. Tung, *Phys. Rev. B* **45**, 13509 (1992).

¹¹I. Ohdomari and K. N. Tu, *J. Appl. Phys.* **51**, 3735 (1980).

¹²S. M. Sze and K. K. Ng, *Physics of Semiconductor Devices* (Wiley, Hoboken, NJ, 2007).

¹³D. G. Pierce and P. G. Brusius, *Microelectron. Reliab.* **37**, 1053 (1997).

¹⁴R. Waser and M. Aono, *Nature Mater.* **6**, 833 (2007).

¹⁵T. Shimizu, N. Gotoh, N. Shinozaki, and H. Okushi, *Appl. Surf. Sci.* **117**, 400 (1997).

¹⁶J. Robertson and C. W. Chen, *Appl. Phys. Lett.* **74**, 1168 (1999).